

## Photochemistry of Ruthenium Trisbipyridine Functionalized on Gold Nanoparticles

P. Pramod,<sup>†</sup> P. K. Sudeep,<sup>†,‡</sup> K. George Thomas,<sup>\*,†</sup> and Prashant V. Kamat<sup>‡</sup>*Photosciences and Photonics, Regional Research Laboratory (CSIR), Trivandrum 695 019, India, and Notre Dame Radiation Laboratory and the Department of Chemistry and Biochemistry, University of Notre Dame, Notre Dame, Indiana 46556-0579**Received: July 31, 2006; In Final Form: September 1, 2006*

Design of nanohybrid systems possessing several ruthenium trisbipyridine ( $\text{Ru}(\text{bpy})_3^{2+}$ ) chromophores on the surface of gold nanoparticles, by adopting a place exchange reaction, was reported and their photophysical properties were tuned by varying the density of chromophores. The charge shift between the excited and ground-state  $\text{Ru}(\text{bpy})_3^{2+}$  chromophores was reported for the first time, leading to the formation of  $\text{Ru}(\text{bpy})_3^+$  and  $\text{Ru}(\text{bpy})_3^{3+}$ . Electron-transfer products were not observed on decreasing the concentration of  $\text{Ru}(\text{bpy})_3^{2+}$  functionalized on Au nanoparticles or in a saturated solution of unbound chromophores. The close proximity of the chromophores on periphery of the gold core may lead to an electron transfer reaction and the products sustained for several nanoseconds before undergoing recombination, probably due to the stabilizing effect of the polar ethylene glycol moieties embedded between the chromophore groups.

## Introduction

The multifaceted properties of matter in the nanoscale dimension offer a wide range of research and development possibilities in diverse areas of photonics, electronics, material science, catalysis, and biology.<sup>1–6</sup> These possibilities have initiated a plethora of activities in the area of nanoscience, particularly the investigations of the physical and chemical properties of matter as it evolves from atoms/molecules to materials.<sup>1,3,5,6</sup> However probing these properties in the nanoscale is still a major challenge. An in-depth understanding on the optical as well as electronic properties of nanoparticles is essential for designing nanophotonic devices.<sup>5,6</sup> It has been demonstrated by our group<sup>3,7</sup> and others<sup>8–12</sup> that the chromophores functionalized onto the metal nanoparticles are best suited for probing their physical properties. Recent studies on chromophore-functionalized metal nanoparticles have revealed several interesting observations: (i) retention of the emission of chromophores when functionalized on gold nanoparticles<sup>3,7,9,12</sup> (it was generally believed that the emission of chromophore is totally quenched on the surface of metals through an energy transfer mechanism<sup>13</sup>), (ii) size dependent electron/energy transfer processes in metal nanoparticles,<sup>3,10,11</sup> and (iii) their ability to store and shuttle electrons.<sup>3,14</sup> Such functionalized nanoparticles are useful as elements in nanophotonic devices and hence it is essential to develop methodologies for incorporating a desired number of chromophores for tuning their optical properties. To investigate this aspect, we have selected one of the most versatile chromophoric systems, namely ruthenium trisbipyridine,  $[\text{Ru}(\text{bpy})_3^{2+}]$ , which is often called as the “king of inorganic complexes”.<sup>15</sup> The photochemical as well as photophysical properties of ruthenium polypyridine systems are well documented,<sup>15,16</sup> and this class of molecule has been

extensively utilized for solar energy harvesting<sup>17,18</sup> and other device applications.<sup>19,20</sup> A few approaches have been reported<sup>21–27</sup> in the literature for assembling ruthenium polypyridines on to Au nanoparticles; however, the rich photochemistry of this class of hybrid systems has not been well exploited. This manuscript presents an effective approach for varying the concentrations of  $\text{Ru}(\text{bpy})_3^{2+}$  chromophore on to the surface of gold nanoparticles and thereby tuning their photophysical properties.

## Results and Discussion

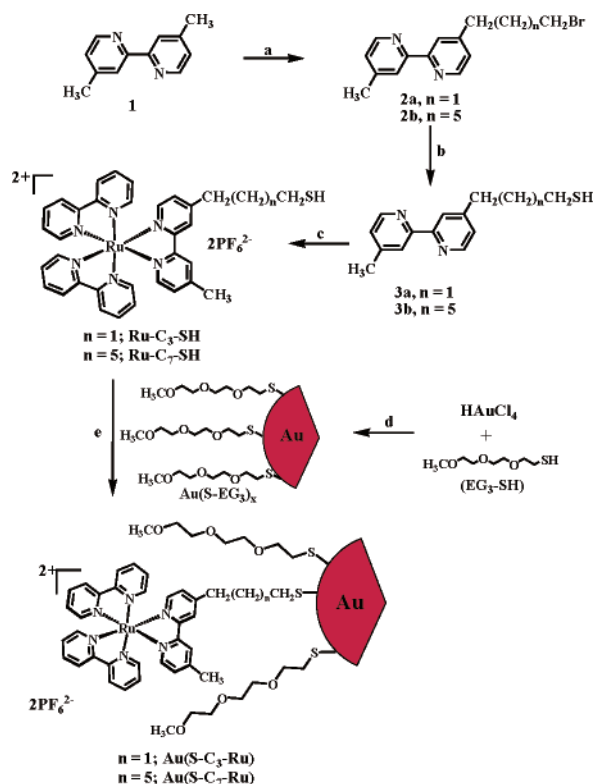
Synthesis of ruthenium thiols,  $\text{Ru}(\text{CH}_2)_3\text{SH}$  and  $\text{Ru}(\text{CH}_2)_7\text{SH}$ , was carried out as per Scheme 1. The monobromoalkyl bipyridine derivatives (**2a** and **2b**) were prepared through a nucleophilic reaction of 4,4'-dimethyl 2,2'-bipyridine with the corresponding  $\alpha,\omega$ -dibromoalkanes, using lithium diisopropylamine as the base.<sup>28</sup> The corresponding bromo derivatives were converted to thiols by reacting with a mixture of tetrabutylammonium fluoride and hexamethyldisilathiane, following a general method reported by Fox and co-workers<sup>29</sup> for the synthesis of thiols. The thiol derivatives were further complexed with  $\text{Ru}(\text{bpy})_2\text{Cl}_2$ , by adopting a general procedure,<sup>30</sup> to yield ruthenium chromophores possessing alkyl spacers of varying chain length (denoted as  $\text{Ru}-\text{C}_3-\text{SH}$  and  $\text{Ru}-\text{C}_7-\text{SH}$ ). Details of the synthesis and characterization of various intermediates and final products are provided as Supporting Information.

The most widely used method for the functionalization of organic molecules on the surface of gold nanoparticles adopts a two-phase synthesis reported by Brust et al.<sup>31</sup> and their modified procedures.<sup>32</sup> Alternatively, metal nanoparticles bearing mixed monolayers can be conveniently synthesized using ligand exchange (place exchange) reactions.<sup>33,34</sup> In the present study we have used octylmercaptan ( $\text{C}_8\text{H}_{17}\text{SH}$ ) as well as monothiol derivative of triethylene glycol ( $\text{EG}_3-\text{SH}$ , Scheme 1) as ligands for preparing monolayer protected gold nanopar-

\* Corresponding author. E-mail: georgetk@md3.vsnl.net.in.

<sup>†</sup> CSIR.

<sup>‡</sup> Notre Dame Radiation Laboratory.

**SCHEME 1. Synthesis of Ru(bpy)<sub>3</sub><sup>2+</sup> Functionalized Gold Nanoparticles**


(a)  $\alpha,\omega$ -dibromoalkane, LDA; (b) hexamethyldisilathiane, tetra-butylammonium fluoride, THF,  $-10^\circ\text{C}$ ; (c) Ru(bpy)<sub>3</sub><sup>2+</sup>, ethanol/water; (d) methanol, NaBH<sub>4</sub>; (e) dichloromethane, rt, 36 h.

ticles (denoted as Au(SC<sub>8</sub>H<sub>17</sub>)<sub>x</sub> and Au(S-EG<sub>3</sub>)<sub>x</sub>,<sup>35a</sup> respectively, where  $x$  indicates the average number of molecules of capping agents).

In the present study, several attempts have been made to functionalize Ru-C<sub>3</sub>-SH/Ru-C<sub>7</sub>-SH onto Au nanoparticle surfaces. The two-phase synthetic procedure adopted by co-binding the chromophores with C<sub>8</sub>H<sub>17</sub>SH, as well as the ligand exchange reaction carried out by reacting with Au(SC<sub>8</sub>H<sub>17</sub>)<sub>x</sub>, were not successful. Both these methods resulted in the precipitation of the nanoparticles which may be due to the noncompatibility of the two molecules on Au surface; the shell of octanethiolate protecting the gold nanoparticles is nonpolar in nature, whereas the Ru(bpy)<sub>3</sub><sup>2+</sup> chromophores are polar in nature. Interestingly, the place exchange reaction with Au(S-EG<sub>3</sub>)<sub>x</sub> possessing the polar triethylene glycol capping agent and Ru-C<sub>3</sub>-SH/Ru-C<sub>7</sub>-SH yielded gold nanoparticles having mixed monolayers denoted as Au(S-EG<sub>3</sub>)<sub>x-y</sub>(S-C<sub>3</sub>-Ru)<sub>y</sub> and Au(S-EG<sub>3</sub>)<sub>x-y</sub>(S-C<sub>7</sub>-Ru)<sub>y</sub> (note: for simplicity of representation, they are abbreviated as Au(S-C<sub>3</sub>-Ru) and Au(S-C<sub>7</sub>-Ru) in the later sections). In a typical synthesis of Au(S-C<sub>7</sub>-Ru), to a stirring solution of Au(S-EG<sub>3</sub>)<sub>x</sub> (0.5 mL, 1.5 mmol) in dichloromethane was added 1 mL solution of Ru-C<sub>7</sub>-SH (5 mg, 3 mmol). The reaction mixture was stirred at room temperature for 36 h. After completion of the reaction, it was centrifuged four times at 4000 rpm, for 5 min each, to remove the unbound Ru-C<sub>7</sub>-SH. Both Au(S-C<sub>3</sub>-Ru) and Au(S-C<sub>7</sub>-Ru) are highly soluble in CH<sub>3</sub>CN and partially soluble in CH<sub>2</sub>-Cl<sub>2</sub>, whereas the starting materials are highly soluble in CH<sub>2</sub>Cl<sub>2</sub>. This allowed the purification of mixed monolayer functionalized gold nanoparticles by first dissolving in CH<sub>2</sub>Cl<sub>2</sub> and then centrifuging. It was confirmed using UV-visible spectroscopic studies that unbound chromophores are absent in the filtrate

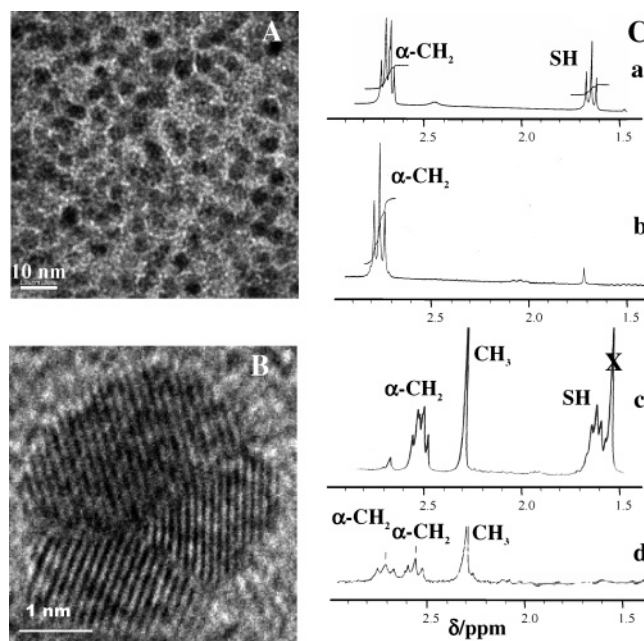


**Figure 1.** (A,B) HRTEM images of Au(S-C<sub>7</sub>-Ru) and (C) <sup>1</sup>H NMR spectra of functionalized gold nanoparticles. (A) Shows an array nanoparticles and (B) illustrates the lattice planes of a single nanoparticle. (C) <sup>1</sup>H NMR spectra of various ligands unbound and bound on Au nanoparticles in the spectral range 1.5–2.6 ppm (crossed peak corresponds to residual water peak in solvent). (a) EG<sub>3</sub>-SH, (b) Au(S-EG<sub>3</sub>)<sub>x</sub>, (c) Ru-C<sub>7</sub>-SH and (d) Au(S-C<sub>7</sub>-Ru) in CD<sub>3</sub>CN.

after the fourth centrifugation. Purified nanoparticles were redispersed in acetonitrile and characterized using high-resolution transmission electron microscopy (HRTEM), <sup>1</sup>H NMR, and UV-visible studies.

The HRTEM samples of Ru(bpy)<sub>3</sub><sup>2+</sup> capped gold nanoparticles were prepared by drop-casting a dilute suspension onto a carbon-coated copper grid. Images presented in Figure 1A indicate the presence of monodispersed gold nanoparticles having an average diameter of 4.5 nm. On this basis we have estimated the number of gold atoms as ~2770 by adopting a tight-packed spherical model suggested by Murray and co-workers.<sup>36</sup> The lattice planes observed in the HRTEM image of the single nanoparticle (Figure 1B) indicate that these nanoparticles are highly crystalline in nature.

To further confirm the surface functionalization of Ru(bpy)<sub>3</sub><sup>2+</sup> chromophores on gold nanoparticles, <sup>1</sup>H NMR spectra of the unbound and bound ligands were recorded. Upon functionalization, significant changes were observed in the spectral range 1.4–3.0 ppm (Figure 1C) where  $\alpha$ -CH<sub>2</sub> and the thiol proton show characteristic peaks, whereas the spectrum remains unchanged in all other regions. The <sup>1</sup>H NMR spectra of EG<sub>3</sub>-SH showed two signals at 1.5 and 2.6 ppm (trace 'a' in Figure 1C); the triplet at 1.6 ppm is attributed to the thiol proton and the doublet of triplet at 2.6 ppm due to  $\alpha$ -CH<sub>2</sub> protons. The thiol protons are not observed for Au(S-EG<sub>3</sub>)<sub>x</sub> confirming the functionalization of EG<sub>3</sub>-SH on to Au nanoparticles and the multiplicity of the  $\alpha$ -CH<sub>2</sub> got reduced to a triplet due to the absence of any interactions with the -SH proton, similar to that reported by Zheng and co-workers.<sup>35a</sup> After the place exchange reaction, the functionalization of Ru(bpy)<sub>3</sub><sup>2+</sup> on the surface of Au nanoparticles was confirmed by the (i) disappearance of thiol proton in Ru-C<sub>7</sub>-SH and (ii) lowering of multiplicity of  $\alpha$ -CH<sub>2</sub> to triplet (as compared to a doublet of triplet in Ru-C<sub>7</sub>-SH), along with a broadening of peaks (trace 'c' and 'd' of Figure 1C). The singlet at 2.3 ppm corresponds

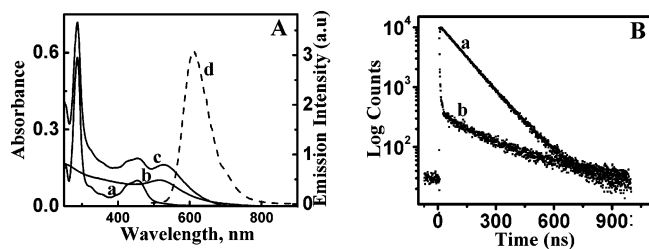


**Figure 2.** Absorption and luminescent lifetime profile of unbound and bound  $\text{Ru}(\text{bpy})_3^{2+}$  on Au nanoparticles in degassed  $\text{CH}_3\text{CN}$ . (A) absorption spectra of (a)  $\text{Ru}-\text{C}_7-\text{SH}$ , (b)  $\text{Au}(\text{S}-\text{EG}_3)_x$ , (c)  $\text{Au}(\text{S}-\text{C}_7-\text{Ru})$ , and the emission spectrum (d) of  $\text{Ru}-\text{C}_7-\text{SH}$ . (B) Luminescence lifetime profile of (a)  $\text{Ru}-\text{C}_7-\text{SH}$  and (b)  $\text{Au}(\text{S}-\text{C}_7-\text{Ru})$ .

to methyl protons of  $\text{Ru}-\text{C}_7-\text{SH}$ . Two factors contribute to the peak broadening upon functionalization: the dipolar spin relaxation and the nonuniform distribution of thiolate ligands on Au nanoparticle surface.<sup>32</sup>

The average number of photoactive molecules per nanoparticle plays a decisive role in tuning the photophysical properties. Place exchange reaction with different proportions of  $\text{Ru}-\text{C}_3-\text{SH}/\text{Ru}-\text{C}_7-\text{SH}$ , enabled us to fix the desired number of  $\text{Ru}(\text{bpy})_3^{2+}$  chromophores around the Au nanoparticles. The average number of chromophores per Au nanoparticles was estimated in conjunction with transmission electron microscopy (TEM), inductively coupled plasma (ICP) analysis and UV-vis absorption spectroscopy (Supporting Information). After the place exchange reaction, the concentration of unreacted chromophore was estimated from the absorption spectra of the filtrate. It was estimated that approximately  $\sim 145$   $\text{Ru}(\text{bpy})_3^{2+}$  chromophores are present on each  $\text{Au}(\text{S}-\text{C}_7-\text{Ru})$  based on the assumption that all the reacted chromophores are evenly distributed on the nanoparticles. Mixed monolayers with lower loading of chromophores ( $\sim 50$  molecules of  $\text{Ru}(\text{bpy})_3^{2+}$  per particle) were prepared by decreasing the concentration of  $\text{Ru}-\text{C}_7-\text{SH}$  used for place exchange reaction, and these samples are denoted as  $\text{Au}(\text{S}-\text{C}_7-\text{Ru})_L$ .

For various steady-state and time-resolved investigations, a degassed solution of ruthenium tris-bipyridine functionalized on gold nanoparticles was used. Absorption spectra of  $\text{Ru}-\text{C}_3-\text{SH}/\text{Ru}-\text{C}_7-\text{SH}$  in acetonitrile possess two bands; one centered around 288 nm attributed to the  $\pi-\pi^*$  transition of bipyridine ligands and other at 453 nm due to the metal-to-ligand charge transfer (MLCT) band (trace 'a' in Figure 2A). The absorption spectral features of  $\text{Ru}-\text{C}_7-\text{SH}$  and surface plasmon band of  $\text{Au}(\text{S}-\text{EG}_3)_x$  (trace 'b') are more or less retained in the case of  $\text{Au}(\text{S}-\text{C}_7-\text{Ru})$ , ruling out the possibility of any strong ground-state interaction (trace 'c'). Similar results were observed for  $\text{Au}(\text{S}-\text{C}_3-\text{Ru})$ . The corresponding emission spectra of both the compounds are centered at 612 nm (trace 'a') and the luminescence quantum yield was estimated as 0.07 (error limit  $\pm 5\%$ ) using  $\text{Ru}(\text{bpy})_3^{2+}$  as standard ( $\Phi_{\text{em}}$  for  $\text{Ru}(\text{bpy})_3^{2+} = 0.084$ ).<sup>37</sup> The spectral properties are summarized in the Supporting Information. Due to the spectral overlap of the plasmon absorption of the nanoparticles with the MLCT band of  $\text{Ru}(\text{bpy})_3^{2+}$ , it was difficult to evaluate the quantum yield of emission of  $\text{Au}(\text{S}-\text{C}_7-\text{Ru})$  and hence the fate of the excited state was elucidated by using luminescent lifetime and nanosecond transient absorption studies.

Unbound  $\text{Ru}-\text{C}_7-\text{SH}$  in various solvents follows monoexponential decay, with a lifetime ( $\tau$ ) of 1.109  $\mu\text{s}$  in  $\text{CH}_2\text{Cl}_2$  and 961 ns in  $\text{CH}_3\text{CN}$ , which is attributed to the inherent lifetime of the chromophore (for example, trace 'a' in Figure 2B). Interestingly,  $\text{Ru}(\text{bpy})_3^{2+}$  functionalized on gold nanoparticles follows biexponential decay in  $\text{CH}_2\text{Cl}_2$  ( $\epsilon = 9.8$ ) with a long-

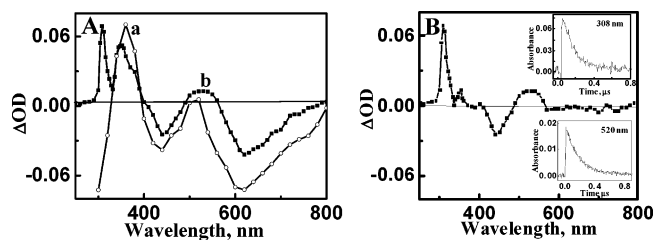


**Figure 3.** Nanosecond transient absorption spectrum (355 nm laser pulse) of unbound and bound  $\text{Ru}(\text{bpy})_3^{2+}$  on Au nanoparticles in  $\text{CH}_3\text{CN}$ . (A) Degassed solution of (a)  $\text{Ru}-\text{C}_7-\text{SH}$  and (b)  $\text{Au}(\text{S}-\text{C}_7-\text{Ru})$  and (B) oxygenated solution of  $\text{Au}(\text{S}-\text{C}_7-\text{Ru})$  and the inset of B shows the absorption-time profile.

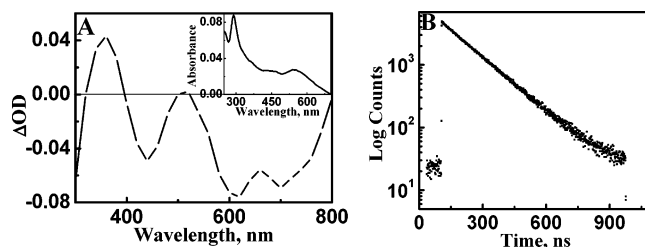


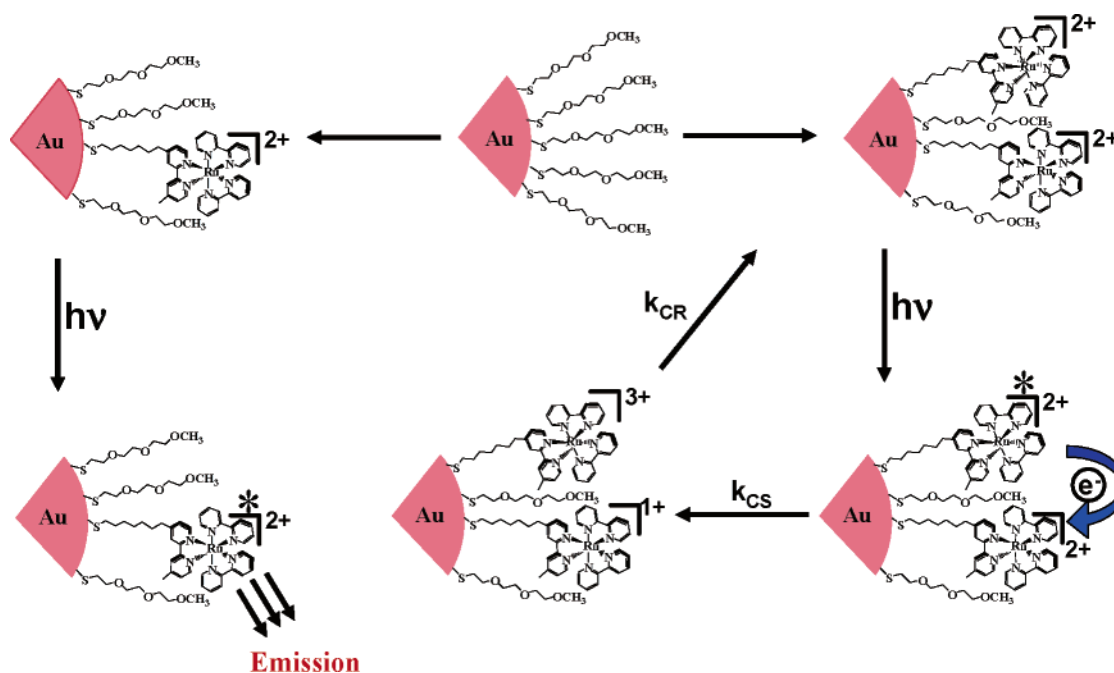
**Figure 4.** (A) Nanosecond transient absorption spectrum (355 nm laser pulse) of  $\text{Ru}(\text{bpy})_3^{2+}$  bound on Au nanoparticles having low loading of chromophore ( $(\text{Au}(\text{S}-\text{C}_7-\text{Ru})_L)$  in degassed  $\text{CH}_3\text{CN}$  solution; inset shows the absorption spectrum. (B) the corresponding luminescence lifetime profile.

lived ( $\tau_1 = 1.10 \mu\text{s}$ ;  $\chi_1 = 80\%$ ) and short-lived ( $\tau_2 = 4.3 \text{ ns}$ ;  $\chi_2 = 20\%$ ) component. The lifetime of the long-lived component (same as that of unbound  $\text{Ru}-\text{C}_7-\text{SH}$ ) can be attributed to the unquenched  $\text{Ru}(\text{bpy})_3^{2+}$  chromophore bound on to gold nanoparticles and the short-lived component to the quenched excited state of  $\text{Ru}(\text{bpy})_3^{2+}$  either through an energy or electron-transfer process. In polar solvent such as  $\text{CH}_3\text{CN}$  ( $\epsilon = 39.8$ ), the relative abundance of the short-lived component substantially increased ( $\tau_1 = 960 \text{ ns}$ ;  $\chi_1 = 30\%$  and  $\tau_2 = 4.3 \text{ ns}$ ;  $\chi_2 = 70\%$ ), further supporting an electron-transfer quenching process (trace 'b' in Figure 2B).

Nanosecond laser flash photolysis was carried out for obtaining a better understanding of the mechanism of the quenching process (Figures 3 and 4A). The difference absorption spectrum recorded following a 355 nm laser excitation of  $\text{Ru}-\text{C}_7-\text{SH}$  in degassed  $\text{CH}_3\text{CN}$  solution possesses a well defined band at 370 nm, which is readily quenched in oxygenated solution. This absorption band is characteristic of the triplet-triplet absorption of  $\text{Ru}(\text{bpy})_3^{2+}$  (trace 'a' in Figure 3A), and the absorption-time profile monitored at 370 nm follows a monoexponential decay with a lifetime of 909 ns ( $k_T = 1.10 \times 10^6 \text{ s}^{-1}$ ).

The corresponding bleach around 450 and 620 nm is attributed to the loss of ground-state absorption and emission, respectively. Interestingly, upon binding onto metal nanoparticles ( $\text{Au}(\text{S}-\text{C}_7-\text{Ru})$ ), two additional bands were observed at 308 and 520 nm along with triplet absorption band (trace 'b' in Figure 3A). The absorption-time profile monitored at 308 nm as well as 520 nm follows monoexponential decay with the same rate constant  $7.4 \times 10^6 \text{ s}^{-1}$  ( $\tau = 135 \text{ ns}$ ), suggesting that both the species originate from the same process. The presence of oxygen has no major effect on the formation and decay of these transients, whereas the triplet absorption band was totally quenched (Figure 3B). Similar results were observed for  $\text{Au}(\text{S}-\text{C}_3-\text{Ru})$  and presented as Supporting Information. Based on these results and spectroelectrochemical studies by Lomoth



SCHEME 2. Light-Induced Processes in  $\text{Au}(\text{S}-\text{C}_7\text{-Ru})$  and  $\text{Au}(\text{S}-\text{C}_7\text{-Ru})_{\text{L}}$ 

et al.,<sup>38</sup> the transients at 308 and 520 nm are assigned as  $\text{Ru}(\text{bpy})_3^{3+}$  and  $\text{Ru}(\text{bpy})_3^+$  arising from a light-induced electron-transfer process between the excited state and ground-state molecules of  $\text{Ru}(\text{bpy})_3^{2+}$  anchored on the surface of gold nanoparticles. Photoinduced charge-transfer interaction between  $\text{Ru}(\text{bpy})_3^{2+}$  chromophores and Au nanoparticles is not observed in the present case, which may be due to the large diameter of Au core ( $> 4.5$  nm). It is well established that the quantum size effects in Au nanoparticles are observed only when the diameter is  $< 3.0$  nm.<sup>39</sup>

The nanohybrid system can be visualized as a core-shell system (Scheme 2) possessing several  $\text{Ru}(\text{bpy})_3^{2+}$  chromophores at the periphery of Au nanoparticles in which the light-induced electron transfer generates a high local concentration of oxidized and reduced products. Interestingly, electron transfer products sustained for several nanoseconds before undergoing recombination, probably due to the stabilizing effect of the polar ethylene glycol moieties embedded between the chromophoric groups. The density of  $\text{Ru}(\text{bpy})_3^{2+}$  chromophores in the monolayer was further estimated, and details are provided as Supporting Information. In the case of  $\text{Au}(\text{S}-\text{C}_7\text{-Ru})$ , 65% of the volume of the shell is occupied by the chromophore. Such dense packing of  $\text{Ru}(\text{bpy})_3^{2+}$  results in formation of oxidized-reduced products on photoexcitation (Figure 3). Interestingly, the chromophore occupies only 23% of the total shell volume in the case of  $\text{Au}(\text{S}-\text{C}_7\text{-Ru})_{\text{L}}$ , and electron-transfer products are not observed (Figure 4). Blank experiments carried out using a saturated solution of  $\text{Ru}-\text{C}_7\text{-SH}$  in the absence and presence of  $\text{EG}_3\text{-SH}$  do not produce any redox products, further confirming the role of gold nanoparticles. To the best of our knowledge, this is the first observation of a light-induced charge shift between a excited as well as ground-state  $\text{Ru}(\text{bpy})_3^{2+}$  chromophores leading to the formation of redox products. Both luminescence and nanosecond transient absorption studies of  $(\text{Au}(\text{S}-\text{C}_7\text{-Ru}))_{\text{L}}$  showed spectral behavior similar to that of  $\text{Ru}-\text{C}_7\text{-SH}$ , and no electron-transfer products were observed on decreasing the concentration of  $\text{Ru}(\text{bpy})_3^{2+}$  (Figure 4). These results clearly indicate that the local concentration of the chromophores plays a decisive role in modulating the photophysics of the  $\text{Ru}(\text{bpy})_3^{2+}$ .

In conclusion, we present an efficient approach for functionalizing  $\text{Ru}(\text{bpy})_3^{2+}$  molecules on Au nanoparticles and demonstrate light-mediated charge shift between the anchored chromophores at higher concentrations. The electron-transfer products, namely  $\text{Ru}(\text{bpy})_3^{3+}$  and  $\text{Ru}(\text{bpy})_3^+$ , were characterized using transient absorption studies and found to be stable for several nanoseconds. Blank experiments clearly indicate the role of core-shell systems in light-induced charge shift. The luminescent properties of  $\text{Ru}(\text{bpy})_3^{2+}$  were retained by lowering the concentration of the chromophore on gold nanoparticles, and such hybrid systems could be further extended for the development of photocatalysts as well as chemical and biological sensors.

**Acknowledgment.** The authors (K.G.T. and P.P.) thank the Department of Science and Technology, Government of India (SP/S5/NM-75/2002) and the Council of Scientific and Industrial Research (CMM 220239) for financial support and (P.V.K. and P.K.S.) thank the Office of the Basic Energy Sciences of the U.S. Department of Energy. This is contribution No. RRLT-PPD-227 from the Regional Research Laboratory (Council of Scientific and Industrial Research), Trivandrum, India and contribution no. NDRL#4679 from the Notre Dame Radiation Laboratory.

**Supporting Information Available:** Detailed synthetic procedures, estimation of number of ruthenium chromophores on the surface of Au nanoparticles, the photophysical properties of bound and unbound  $\text{Ru}-\text{C}_3\text{-SH}/\text{Ru}-\text{C}_7\text{-SH}$ . This material is available free of charge via the Internet at <http://pubs.acs.org>.

## References and Notes

- (1) Rao, C. N. R.; Kulkarni, G. U.; Thomas, P. J.; Edwards, P. P. *Chem.-Eur. J.* **2002**, *8*, 29.
- (2) Shenhar, R.; Rotello, V. M. *Acc. Chem. Res.* **2003**, *36*, 549.
- (3) Thomas, K. G.; Kamat, P. V. *Acc. Chem. Res.* **2003**, *36*, 888.
- (4) Katz, E.; Shipway, A. N.; Willner, I. In *Nanoscale Materials*; Liz-Marzan, L. M., Kamat, P. V., Eds.; Kluwer Academic Publishers: Boston, **2003**; pp 5-78.
- (5) Daniel, M.-C.; Astruc, D. *Chem. Rev.* **2004**, *104*, 293.

- (6) Burda, C.; Chen, X.; Narayanan, R.; El-Sayed, M. A. *Chem. Rev.* **2005**, *105*, 1025.
- (7) Ipe, B. I.; Thomas, K. G. *J. Phys. Chem. B* **2004**, *108*, 13265.
- (8) Fan, C. H.; Wang, S.; Hong, J. W.; Bazan, G. C.; Plaxco, K. W.; Heeger, A. J. *Proc. Natl Acad. Sci. U.S.A.* **2003**, *100*, 6297.
- (9) Stellacci, F.; Bauer, C. A.; Meyer-Friedrichsen, T.; Wenseleers, W.; Marder, S. R.; Perry, J. W. *J. Am. Chem. Soc.* **2003**, *125*, 328.
- (10) Chen, M. M. Y.; Katz, A. *Langmuir* **2002**, *18*, 2413.
- (11) Dulkeith, E.; Morteani, A. C.; Niedereichholz, T.; Klar, T. A.; Feldmann, J.; Levi, S. A.; van Veggel, F. C. J. M.; Reinhoudt, D. N.; Moller, M.; Gittins, D. I. *Phys. Rev. Lett.* **2002**, *89*, 203002.
- (12) Imahori, H.; Arimura, M.; Hanada, T.; Nishimura, Y.; Yamazaki, I.; Sakata, Y.; Fukuzumi, S. *J. Am. Chem. Soc.* **2001**, *123*, 335.
- (13) Drexhage, K. H.; Kuhn, H.; Shafer, F. P. *Ber. Bunsen-Ges. Phys. Chem.* **1968**, *72*, 329.
- (14) Hirakawa, T.; Kamat, P. V. *J. Am. Chem. Soc.* **2005**, *127*, 3928.
- (15) Juris, A.; Balzani, V.; Barigelli, F.; Campagna, S.; Belser, P.; von Zelewsky, A. *Coord. Chem. Rev.* **1988**, *84*, 85.
- (16) McCusker, J. K. *Acc. Chem. Res.* **2003**, *36*, 876.
- (17) Hagfeldt, A.; Gratzel, M. *Acc. Chem. Res.* **2000**, *33*, 269.
- (18) Wang, Q.; Zakeeruddin, S. M.; Nazeeruddin, M. K.; Humphry-Baker, R.; Gratzel, M. *J. Am. Chem. Soc.* **2006**, *128*, 4446.
- (19) Miao, W.; Choi, J. P.; Bard, A. J. *J. Am. Chem. Soc.* **2002**, *124*, 14478.
- (20) Clarke, Y.; Xu, W.; Demas, J. N.; DeGraff, B. A. *Anal. Chem.* **2000**, *72*, 3468.
- (21) Akiyama, T.; Inoue, K.; Kuwahara, Y.; Niidome, Y.; Terasaki, N.; Nitahara, S.; Yamada, S. *Langmuir* **2005**, *21*, 793.
- (22) Terasaki, N.; Otsuka, K.; Akiyama, T.; Yamada, S. *Jpn. J. Appl. Phys. Part 1* **2004**, *43*, 2372.
- (23) Ito, M.; Tsukatani, T.; Fujihara, H. *J. Mater. Chem.* **2005**, *15*, 960.
- (24) Dong, T. Y.; Shih, H. W.; Chang, L. S. *Langmuir* **2004**, *20*, 9340.
- (25) Glomm, W. R.; Moses, S. J.; Brennaman, M. K.; Papanikolas, J. M.; Franzen, S. *J. Phys. Chem. B* **2005**, *109*, 804.
- (26) Huang, T.; Murray, R. W. *Langmuir* **2002**, *18*, 7077.
- (27) Xu, X. H. N.; Huang, S.; Brownlow, W.; Salaita, K.; Jeffers, R. B. *J. Phys. Chem. B* **2004**, *108*, 15543.
- (28) Salmon, L.; Verlhac, J.-B.; Bied-Charreton, C.; Verchère-Béaur, C.; Gaudemer, A.; Pasternack, R. F. *Tetrahedron Lett.* **1990**, *31*, 519.
- (29) Hu, J.; Fox, M. A. *J. Org. Chem.* **1999**, *64*, 4959.
- (30) Sullivan, B. P.; Salmon, D. J.; Meyer, T. J. *Inorg. Chem.* **1978**, *17*, 3334.
- (31) Brust, M.; Walker, M.; Bethell, D.; Schffrin, D. J.; Whyman, R. *J. Chem. Soc., Chem. Commun.* **1994**, 801.
- (32) Templeton, A. C.; Wuelfing, W. P.; Murray, R. W. *Acc. Chem. Res.* **2000**, *33*, 27.
- (33) Song, Y.; Murray, R. W. *J. Am. Chem. Soc.* **2002**, *124*, 7096.
- (34) Ionita, P.; Gilbert, B. C.; Chechik, V. *Angew. Chem., Intl. Ed.* **2005**, *44*, 3720.
- (35) (a) A modified procedure (35b) was adopted for the synthesis of Au(S-EG<sub>3</sub>)<sub>x</sub> and details are provided as Supporting Information. (b) Zheng, M.; Li, Z. G.; Huang, X. Y. *Langmuir* **2004**, *20*, 4226.
- (36) (a) Terill, R. H.; Postlethwaite, T. A.; Chen, C.-h.; Poon, C. D.; Terzis, A.; Chen, A.; Hutchison, J. E.; Clark, M. R.; Wignall, G.; Londono, J. D.; Superfine, R.; Falvo, M.; Johnson, C. S., Jr.; Samulski, E. T.; Murray, R. W. *J. Am. Chem. Soc.* **1995**, *117*, 12537. (b) Assigns the gold core as a sphere with density of 58.01 atoms/nm<sup>3</sup> covered with a skin of hexagonally close packed gold atoms with number density of surface gold atoms as 13.89 atoms/nm<sup>2</sup>.
- (37) Goze, C.; Chambron, J.-C.; Heitz, V.; Pomeranc, D.; Salom-Roig, X. J.; Sauvage, J.-P.; Morales, A. F.; Barigelli, F. *Eur. J. Inorg. Chem.* **2003**, 3752.
- (38) Lomoth, R.; Häupl, T.; Johansson, O.; Hammarström, L. *Chem. – Eur. J.* **2002**, *8*, 102.
- (39) Templeton, A. C.; Pietron, J. J.; Murray, R. W.; Mulvaney, P. J. *Phys. Chem. B* **2000**, *104*, 564.